Correlation of Low-Barrier Hydrogen Bonding and Oxyanion Binding in Transition State Analogue Complexes of Chymotrypsin[†,‡,§]

David Neidhart,[||] Yaoming Wei,[||] Constance Cassidy, Jing Lin, W. Wallace Cleland, and Perry A. Frey*

University of Wisconsin−Madison, 1710 University Avenue, Madison, Wisconsin 53705

Received November 3, 2000; Revised Manuscript Received December 22, 2000

ABSTRACT: The structures of the hemiketal adducts of Ser 195 in chymotrypsin with *N*-acetyl-L-leucyl-L-phenylalanyl trifluoromethyl ketone (AcLF-CF_3) and *N*-acetyl-L-phenylalanyl trifluoromethyl ketone (AcF-CF_3) were determined to 1.4−1.5 Å by X-ray crystallography. The structures confirm those previously reported at 1.8−2.1 Å [Brady, K., Wei, A., Ringe, D., and Abeles, R. H. (1990) *Biochemistry 29*, 7600−7607]. The 2.6 Å spacings between Nδ1 of His 57 and Oδ1 of Asp 102 are confirmed at 1.3 Å resolution, consistent with the low-barrier hydrogen bonds (LBHBs) between His 57 and Asp 102 postulated on the basis of spectroscopy and deuterium isotope effects. The X-ray crystal structure of the hemiacetal adduct between Ser 195 of chymotrypsin and *N*-acetyl-L-leucyl-L-phenylalanal (AcLF-CHO) has also been determined at pH 7.0. The structure is similar to the AcLF-CF_3 adduct, except for the presence of two epimeric adducts in the *R*- and *S*-configurations at the hemiacetal carbons. In the (*R*)-hemiacetal, oxygen is hydrogen bonded to His 57, not the oxyanion site. On the basis of the downfield ^{1}H NMR spectrum in solution, His 57 is not protonated at Nϵ2, and there is no LBHB at pH >7.0. Because addition of AcLF-CHO to chymotrypsin neither releases nor takes up a proton from solution, it is concluded that the hemiacetal oxygen of the chymotrypsin−AcLF-CHO complex is a hydroxyl group and not attracted to the oxyanion site. The protonation states of the hemiacetal and His 57 are explained by the high basicity of the hemiacetal oxygen (pK_a > 13.5) relative to that of His 57. The ^{13}C NMR signal for the adduct of AcLF-^{13}CHO with chymotrypsin is consistent with a neutral hemiacetal between pH 7 and 13. At pH <7.0, His 57 in the AcLF-CHO−hemiacetal complex of chymotrypsin undergoes protonation at Nϵ2 of His 57, leading to a transition of the 15.1 ppm downfield signal to 17.8 ppm. The pK_as in the active sites of the AcLF-CF_3 and AcLF-CHO adducts suggest an energy barrier of 6−7 kcal mol^{-1} against ionizations that change the electrostatic charge at the active site. However, ionizations of neutral His 57 in the AcLF-CHO−chymotrypsin adduct, or in free chymotrypsin, proceed with no apparent barrier. Protonation of His 57 is accompanied by LBHB formation, suggesting that stabilization by the LBHB overcomes the barrier to ionization. On the basis of the hydration constant for AcLF-^{13}CHO and its inhibition constant, its K_d is 16 μM, 8000-fold larger than the comparable value for AcLF-CF_3.

Spectroscopic studies of the chemical mechanism of chymotrypsin have led to the proposal that a low-barrier hydrogen bond (LBHB)[1] is formed between Asp 102 and His 57 of the catalytic triad in the transition state for acylation of Ser 195 (*1*−*4*). As part of our continuing effort to test this hypothesis, we have undertaken high-resolution X-ray crystallographic analysis of transition state analogue complexes of chymotrypsin. The primary goal of this study is to determine whether hydrogen bonding distances within the catalytic triad are consistent with the requirements for formation of an LBHB. In addition, we explore the structure of the complex formed by a peptidyl aldehyde inhibitor with chymotrypsin.

The ideal structural analysis would provide highly accurate positions of all the atoms of the catalytic triad, including hydrogen atoms, in the transition state of the enzyme; however, this is beyond the capabilities of any existing experimental method. Neutron diffraction can provide direct visualization of hydrogen atoms; however, in its application to protein structure neutron diffraction is limited to moderate

[†] Supported by Grants GM 30480 and DK 28607 (P.A.F.), GM 51806 (W.W.C.), and DK 47814 (H. M. Holden) from the National Institutes of Health. This study made use of the National Magnetic Resonance Facility at Madison, which is supported by NIH Grant RR02301 from the Biomedical Research Technology Program, National Center for Research Resources. Equipment in the facility was purchased with funds from the University of Wisconsin, the NSF Biological Instrumentation Program (Grant DMB-8415048), the NIH Biomedical Research Technology Program (Grant RR02301), the NIH Shared Instrumentation Program (Grant RR02781), and the U.S. Department of Agriculture.

[‡] The coordinates for the following compounds were deposited in the Protein Data Bank: 1GG6, γ-chymotrypsin with AcF-CF_3; and 1GGD, γ-chymotrypsin with AcLF-CHO.

[§] Contribution from the Department of Biochemistry, University of Wisconsin−Madison.

* To whom correspondence should be addressed: University of Wisconsin−Madison, 1710 University Ave., Madison, WI 53705. Telephone: (608) 262-0055. Fax: (608) 265-2904. E-mail: frey@biochem.wisc.edu.

[||] These authors contributed equally to the research in this article.

[1] Abbreviations: NMR, nuclear magnetic resonance; LBHB, low-barrier hydrogen bond; AcLF-CF_3, *N*-acetyl-L-leucyl-L-phenylalanyl trifluoromethyl ketone; AcF-CF_3, *N*-acetyl-L-phenylalanyl trifluoromethyl ketone; AcLF-CHO, *N*-acetyl-L-leucyl-L-phenylalanal; AcLF-$CH(OH)_2$, hydrate of AcLF-CHO.

10.1021/bi002535a CCC: $20.00
Published on Web 02/02/2001

resolution and requires substitution of deuterium atoms for hydrogen atoms. Unfortunately, in LBHB systems deuterium displays hydrogen bonding characteristics different from those of hydrogen (*5*), and this feature renders neutron diffraction inappropriate for the current study. While hydrogen atoms in proteins are difficult or impossible to visualize with X-ray diffraction, their associated heavier atoms can be localized with great precision. This provides an opportunity to test the hypothesis that an LBHB exists within the catalytic triad of chymotrypsin. Studies of small-molecule model systems have demonstrated that formation of an LBHB between an imidazole group and a carboxyl group requires a distance of less than twice the sum of van der Waals radii for N and O, which is <2.7 Å between appropriate polar atoms (*5*, *6*).

Although the transition state of a reaction is far too fleeting to be observed with routine crystallographic methods, we are fortunate to have access to stable inhibitor complexes that are excellent mimics of the transition state. Both peptidyl trifluoromethyl ketones and peptidyl aldehydes form stable adducts with the active site of chymotrypsin. Peptidyl trifluoromethyl ketone adducts are close structural and electronic analogues of the tetrahedral intermediate in the catalytic mechanism of chymotrypsin. Furthermore, because the tetrahedral intermediate is energetically unstable, the Hammond postulate predicts that the transition state of the enzymatic reaction will closely resemble the tetrahedral intermediate (*7*). Accordingly, we have undertaken high-resolution crystallographic studies of these inhibitor complexes with chymotrypsin to test the hypothesis that an LBHB is formed between Nδ1 of His 57 and Oδ2 of Asp 102 in the transition state of the enzymatic reaction.

High-resolution crystal structures of chymotrypsin adducts with AcF-CF_3 and AcLF-CF_3 at 1.8−2.1 Å resolution have been published, and they showed that the distances between Nδ1 of His 57 and Oδ2 of Asp 102 were 2.5−2.6 Å, consistent with LBHBs (*8*). Because of the importance of these distances with respect to the assignment of LBHBs, we have sought to obtain the structures at a higher resolution. We have extended the study to the adduct of chymotrypsin with AcLF-CHO, which differs with respect to chemical properties from the corresponding trifluoromethyl ketone.

Despite the large body of literature on the interactions of chymotrypsin with both naturally occurring and synthetic inhibitors, there is no reported crystal structure of a complex between chymotrypsin and a peptidyl aldehyde inhibitor. A limited number of previous crystallographic studies have revealed important features of the complexes formed between peptidyl aldehyde inhibitors and related serine proteases. For instance, peptidyl aldehyde inhibitors have been demonstrated to form hemiacetal adducts with *Streptomyces griseus* protease A (*9*, *10*) and with trypsin (*11*). These same studies have demonstrated that the hemiacetal adducts formed with the active site of the enzyme can assume alternative configurations, corresponding to nucleophilic attack of the Ser 195 hydroxyl group upon either the *si* or *re* face of the planar prochiral aldehyde group and producing the *S*- or *R*-configuration at the hemiacetal center of the adducts. This latter result is intriguing because the two configurations of the hemiacetal adduct differ substantially in the location of the hemiacetal oxygen atom.

A fundamental difference between the spectroscopic properties of the adduct of chymotrypsin with AcLF-CHO and the corresponding AcLF-CF_3 is reported here. Inasmuch as interpretation of spectroscopic data for complexes of peptidyl aldehyde inhibitors with chymotrypsin depends critically upon knowledge of the precise mode of binding of these inhibitors, we have undertaken a high-resolution crystallographic study of the complex formed between γ-chymotrypsin and AcLF-CHO.

MATERIALS AND METHODS

Crystal Growth and Inhibition. α-Chymotrypsin was purchased from Sigma (St. Louis, MO), converted to γ-chymotrypsin, and crystallized by large-scale vapor diffusion against 65% saturated ammonium sulfate according to the procedure of Stoddard et al. (*12*). Crystals typically appeared within 1 month and were fully grown by 2 months. Prior to inhibition, crystals of native chymotrypsin were vapor equilibrated for at least 2 days against a synthetic mother liquor consisting of 75% saturated ammonium sulfate and 10 mM potassium phosphate (pH 7.0). Inhibitor soaks with AcF-CF_3, AcLF-CF_3, and AcLF-CHO were prepared by using an acetonitrile cosolvent as described in the previous crystallographic study of Brady et al. (*8*). The crystals were soaked for several months, with addition of more inhibitor and cosolvent after 1 month. The final concentration of each inhibitor was 5 mM in 5% acetonitrile.

Cryocrystallography. Cryoprotectant mother liquor was prepared with increasing concentrations of ethylene glycol up to 15% v/v. To hold the precipitant concentration constant, these soaks were prepared by dilution of concentrated stock solutions and solid ammonium sulfate to yield a final solution of 75% saturated ammonium sulfate and 10 mM potassium phosphate in 5, 10, or 15% (v/v) aqueous ethylene glycol. Crystals were subjected to sequential 5 min soaks in 5, 10, and 15% ethylene glycol cryoprotectant solvents and were then scooped onto a mounted loop of nylon suture and flash-frozen in a −160 °C nitrogen gas cryostream.

Data Collection. X-ray diffraction data were collected with a Siemens X1000D multiwire area detector mounted on a three-axis goniometer. The X-ray source was a Rigaku RU200 rotating anode generator equipped with focusing mirrors. The crystal-to-detector distance was set to14 cm, and 0.15° oscillation frames were accumulated over 1−3 min per frame. A Nicolet LT-1 nitrogen gas cryostream was used for cryotemperature studies; otherwise, crystals mounted in quartz capillaries were cooled to 4 °C with an FPS crystal cooler. The diffraction intensity measurements were integrated with XDS (*13*) and scaled together with XSCALIBRE (G. Wesenberg and I. Rayment, unpublished results). Final unit cell dimensions for each structure were calculated as the average of the XDS global parameter refinement results (GLOREF) for all the individual sweeps of data comprising a data set.

Refinement. PDB entry 2GCH (*14*) was used as the initial model for refinement of the inhibitor complexes against data sets collected at 4 °C. The 2GCH model was stripped of water molecules and subjected to rigid-body refinement followed by least-squares refinement in TNT (*15*). Water molecules and inhibitor molecules were located in difference electron density maps and added to the atomic model.

Table 1: Data Collection and Refinement Statistics of γ-Chymotrypsin Inhibitor Complexes

	AcF-CF_3 (4 °C)	AcF-CF_3 (−160 °C)	AcLF-CF_3 (4 °C)	AcLF-CHO (4 °C)
data statistics				
resolution (Å)	1.4	1.4	1.5	1.5
no. of unique reflections	45939	45082	38699	38043
average redundancy	4.0	3.6	5.3	3.9
R_{sym} (%)	3.0 (17)	2.7 (12)	3.6 (18)	4.3 (18)
completeness (>2σ)	89.8 (59.9)	91.4 (75.8)	94.2 (82.7)	88.0 (55.1)
refinement statistics				
resolution range (Å)	8.0−1.4	8.0−1.4	8.0−1.5	8.0−1.5
no. of reflections (>2σ)	42541	42041	36520	34112
no. of protein atoms	1746	1751	1746	1738
no. of bound waters	228	333	213	215
R_{factor}/R_{free} (%)	17.6/20.5	17.5/21.2	17.2/20.4	18.2/21.2
rms deviations from ideality				
bond lengths (Å)	0.008	0.006	0.008	0.005
bond angles (deg)	1.4	1.4	1.4	1.3

Geometric parameters for the inhibitors were derived from standard libraries and from the small-molecule crystal structure of *N*-acetyl-L-leucine-D,L-phenylalanine trifluoromethyl ketone (D. Powell, unpublished data); the small-molecule crystal structure coordinates for this compound are included in footnotes describing the PDB entries of the refined chymotrypsin−inhibitor complexes. Further refinement of the 4 and −160 °C complexes was performed using energy minimization and simulated annealing in XPLOR (*16*). The initial model for the −160 °C complex structure was derived from the partially refined 4 °C structure of the complex between chymotrypsin and AcF-CF_3. The model was stripped of water and inhibitor molecules and subjected to rigid-body refinement prior to further refinement in XPLOR. Statistics on X-ray data collection and refinement of inhibitor complexes of γ-chymotrypsin are summarized in Table 1.

Synthesis of Chymotrypsin Inhibitors. AcF-CF_3 and AcLF-CF_3 were synthesized as previously described (*17*). AcLF-CHO was prepared from the phenylalanine methyl ester and *N*-acetyl-L-leucine as described previously (*18*). L-[1-^{13}C]-Phenylalanine was purchased from Isotec Inc., protected as its methyl ester by reaction in methanol saturated with hydrochloric gas, and used for the synthesis of AcLF−^{13}CHO.

pH Titrations of Chymotrypsin−AcLF-CHO Complexes. Solutions of chymotrypsin (2 mM) were prepared in 0.5 M buffers at pHs ranging from 4.5 to 13 using acetate, MES, phosphate, and carbonate buffers. AcLF-CHO was dissolved in DMSO-d_6 to make a 100 mM stock solution, which was added in microliter aliquots to the chymotrypsin samples, such that the total inhibitor concentration was 5 mM, ensuring that most of the chymotrypsin was present as the hemiacetal adduct with the inhibitor. DMSO-d_6 was 5% (v/v) in the solution and was used as the lock signal.

All NMR spectra were acquired with 5 mm NMR tubes on a 500 MHz Bruker spectrometer at 5 °C. ^{1}H NMR spectra were acquired using a TXI probe and a nonsaturating water signal suppression program (*19*). Spectral conditions were 8000 time domain points and 8000 scans. The data were processed at a Silicon Graphics workstation using the Felix95 software package. The exponential line broadening was set to 20 Hz. Baselines were corrected with a fifth-order polynomial. All chemical shifts were referred to sodium 3-(trimethylsilyl)-1-propanesulfonate.

Hydration Constant for AcLF-CHO. NMR spectra were acquired using 5 mM AcLF-^{13}CHO in 0.1 M phosphate buffer (pH 7.8), containing 5% DMSO-d_6, at 25 °C. The areas of the aldehyde and hydrate signals were quantitated, by both the integration and the cut-and-weigh method. The hydration constant K_h was calculated by dividing the area of the hydrate signal by that of the aldehyde.

RESULTS

Structures of Peptidyl Trifluoromethyl Ketone Adducts. The structures of the adducts of AcLF-CF_3 and AcF-CF_3 with γ-chymotrypsin are generally consistent with the results of the earlier study of Brady et al. (*8*). The improved resolution of the current study permits more accurate determination of atomic positions and interatomic distances, especially the critical hydrogen bonding distances within the catalytic triad. The electron density maps produced by this study have strong, continuous electron density between the side chain oxygen atom of Ser 195 and the inhibitors (Figures 1 and 2). This demonstrates formation of covalent hemiketal linkages with the active site of the enzyme.

A surprising feature of the high-resolution crystal structure of the AcF-CF_3 chymotrypsin adduct was the discovery of an auxiliary binding site for the inhibitor, located at a crystal packing contact between molecules of chymotrypsin. This second molecule of the inhibitor lacks any covalent attachment to the enzyme, and appears to be bound primarily through lipophilic contact. As the interface between chymotrypsin molecules that forms this auxiliary binding pocket is enforced by the crystalline lattice, and there is no evidence that chymotrypsin is active as a dimer in solution, it is unlikely that this binding pocket has any functional significance. In addition, there is very little electron density at this site in the γ-chymotrypsin−AcLF-CF_3 complex, indicating that the latter inhibitor binds weakly at this site, if at all. Aside from rotation of a few solvent-exposed side chains, binding of AcF-CF_3 at this auxiliary binding site does not appear to produce any large-scale structural changes in chymotrypsin.

Hydrogen Bonding Distances. As listed in Table 2, the distance between His 57 and Asp 102 is 2.6 Å in each of the trifluoromethyl ketone adduct structures. The mean coordinate error in crystal structures may be estimated from the trend in the disagreement between measured and

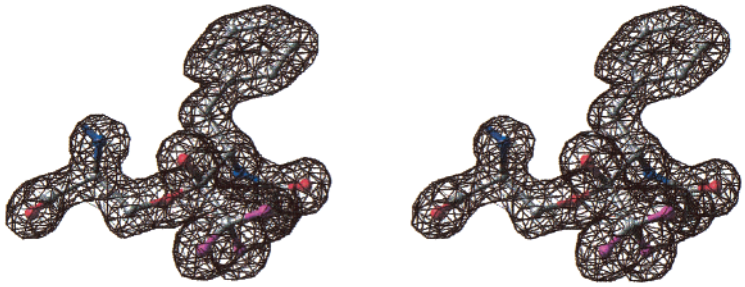

FIGURE 1: Electron density and atomic model of the AcF-CF_3 adduct of chymotrypsin. An $F_o - F_c$ "omit" electron density map is displayed in black with a stick figure of Ser 195 and the inhibitor adduct colored as follows: carbon, gray; oxygen, red; nitrogen, blue; and fluorine, violet. Ser 195 and the inhibitor were excluded from the map calculation. The map is contoured at 4σ. Note the continuous electron density between Ser 195 and the inhibitor.

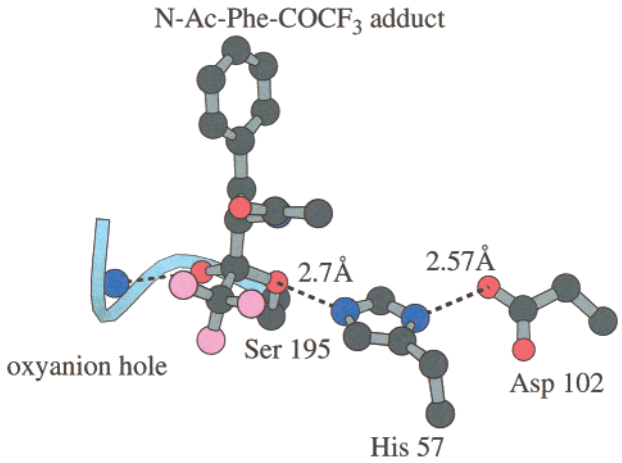

FIGURE 2: Atomic model of the AcF-CF_3 adduct with hydrogen bonding distances.

Table 2: His 57 to Asp 102 Hydrogen Bonding Distances in γ-Chymotrypsin Inhibitor Complexes

	AcF-CF_3 (4 °C)	AcF-CF_3 (−160 °C)	AcLF-CF_3 (4 °C)	AcLF-CHO (4 °C)
H-bonding distance (Å)	2.61	2.57	2.61	2.62

calculated structure factor magnitudes as a function of resolution according to the method of Luzzati (*20*). These calculations lead to an estimate of about 0.15 Å as the mean uncertainty of the atomic positions in these crystal structures.

Thus, by any reasonable statistical criteria, we have not proved that an LBHB exists on the basis of distance criteria; rather, we have failed to disprove it. However, several points should be borne in mind. First, the mean uncertainty in atomic positions estimated from the Luzatti plot includes all atoms in the atomic model, including atoms of surface residues that are highly mobile and therefore have high positional uncertainties. Many of these residues may alternate between different discrete conformations, only some of which have been included in the current atomic model. In contrast, the atoms of the inhibitor and active site are extremely well defined by the electron density (Figure 1), and are likely to have an uncertainty far less than the mean. In addition, in the interest of providing the most stringent test of the hypothesis that an LBHB exists in these complexes, we left the van der Waals repulsive terms between atoms at full force in the XPLOR refinement; no effort was made to reduce or eliminate these terms either locally for the atoms of the catalytic triad or globally throughout the protein. Since an LBHB requires a distance between His 57 Nδ1 and Asp 102 Oδ2 that is less than the sum of their van der Waals radii, this effectively biases the experiment toward the null hypothesis. In contrast, we observe that the X-ray diffraction data from these complexes have overwhelmed this opposing bias and have consistently produced a result that is in agreement with the requirements for formation of an LBHB.

Structure of the Chymotrypsin−AcLF-CHO Adduct. As observed for the trifluoromethyl ketone complexes, the electron density maps of the chymotrypsin−AcLF-CHO complex have strong, continuous electron density between the side chain oxygen atom of Ser 195 and the inhibitor (Figure 3). This demonstrates formation of a covalent hemiacetal linkage with the active site of the enzyme. Crystal structures of the complexes of peptidyl aldehyde inhibitors with other serine proteases have yielded similar results (*10*, *11*).

During refinement of the adduct formed between chymotrypsin and AcLF-CHO, it quickly became apparent that the adduct could not adequately be modeled by a single configuration of the hemiacetal oxygen atom. Rather, the hemiacetal oxygen atom is split between two configurations, corresponding to the *R*- and *S*-stereoisomers of the hemiacetal adduct. In the *S*-configuration, the hemiacetal oxygen atom occupies the "oxyanion hole" of chymotrypsin and is within hydrogen bonding distance of the backbone NH groups of Gly 193 and Ser 195 (Figure 4a). In the *R*-configuration, the hemiacetal oxygen occupies a position within hydrogen bonding distance of the imidazole group of His 57 (Figure 4b). Similar bifurcation of the hemiacetal oxygen atom has been observed in the crystal structure of the adduct formed between trypsin and leupeptin (*11*) and between *S. griseus* protease A and chymostatin (*9*, *10*).

The observation that the hemiacetal oxygen is within hydrogen bonding distance of His 57 in the *R*-configuration of the adduct has important implications that are brought into focus by spectroscopic and chemical results in the following sections.

Inhibition of Chymotrypsin by AcLF-CHO. The observed inhibition constant for this inhibitor was reported to be 17.7 μM (*21*). The reported value of K_i was computed on the basis of the total inhibitor concentration, including both the aldehyde hydrate and aldehyde species, but only the aldehyde form binds effectively (*22*). The measured value of K_i can be used to obtain the dissociation constant K_d for the aldehyde species if the hydration constant is known (*23*). Therefore, we synthesized AcLF-^{13}CHO and used it to measure the hydration constant in water.

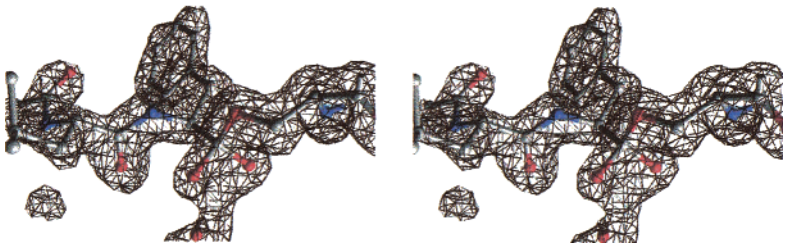

FIGURE 3: Electron density and atomic model of the AcLF-CHO adduct of chymotrypsin. An omit $F_o - F_c$ electron density map and atomic model of the AcLF-CHO adduct displayed as in Figure 1. Ser 195 and the inhibitor were excluded from the map calculation. The map is contoured at 4σ. Note the continuous electron density between Ser 195 and the inhibitor.

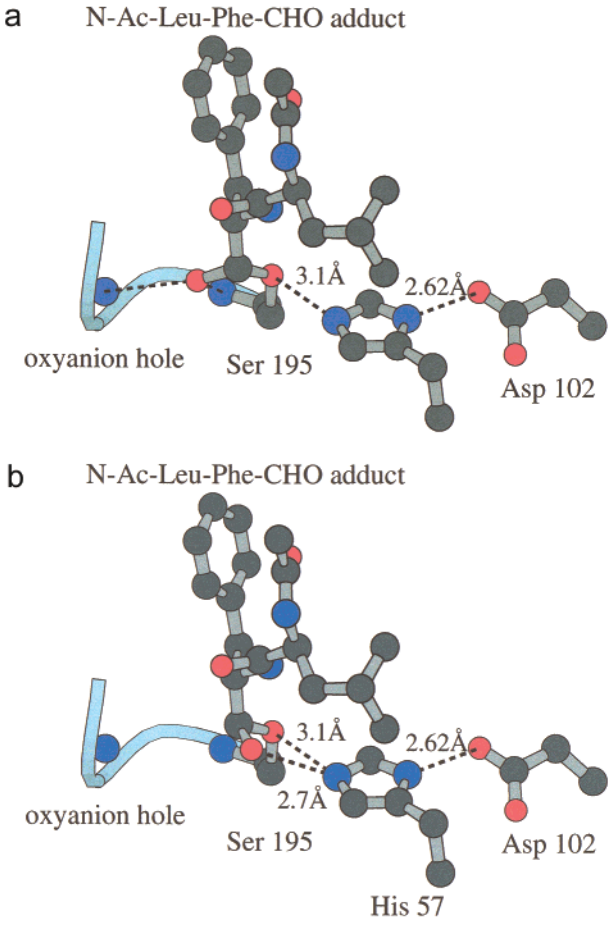

FIGURE 4: Atomic models for the *S*- and *R*-configurations of the AcLF-CHO adduct with hydrogen bonding distances. (a) In the *S*-configuration, the hemiacetal oxygen resides in the oxyanion site. (b) In the *R*-configuration, the hemiacetal oxygen no longer resides in the oxyanion site, but instead is within hydrogen bonding distance of the Nϵ1 atom of His 57.

In chloroform solution, AcLF-^{13}CHO displays a single ^{13}C resonance at 199.6 ppm, corresponding to the aldehyde species. When AcLF-^{13}CHO is dissolved in aqueous solution at pH 7.8, two resonances appear at 204.2 and 92.9 ppm, corresponding to the aldehyde and its hydrate, respectively. The ratio of hydrate to aldehyde is ~10; that is, the hydration constant K_d is 10 ± 1, referring to unit activity for water. This value is consistent with that previously reported for another aldehyde (*22*).

The value of K_d for AcLF-CHO as an inhibitor of chymotrypsin can be computed with the equation $K_d = K_i/(1 + K_h)$, where K_i is the inhibition constant and K_h is the hydration constant. Substituting values of 17.7 μM for K_i and 10 for K_d, we calculate a K_d of 1.6 μM. The comparable value for the trifluoromethyl ketone inhibitor AcLF-CF_3 is 0.2 nM, based on inhibition data (*17*) and the hydration constant for this inhibitor (*24*). Therefore, the keto form of AcLF-CF_3 binds to chymotrypsin 8000-fold better than the aldehyde form of AcLF-CHO, which corresponds to a difference of 5.5 kcal mol^{-1} in the free energy of binding. A substantial part of this difference can be attributed to the electrophilic reactivity of trifluoromethyl ketones relative to aldehydes, as represented by the 450-fold difference in hydration constants.

Ionization of AcLF-CH(OH)$_2$. A pK_a value for a hemiacetal of AcLF-CHO would be of value for interpreting the structure of its adduct with Ser 195 in chymotrypsin. Ionization of a hemiacetal proved to be difficult to observe, owing to its high basicity and the sensitivity of AcLF-CHO in basic solutions. Therefore, the pK_a of AcLF-^{13}CH(OH)$_2$ was measured as an initial model for the ionization of a hemiacetal. The inhibitor was dissolved in solutions with increasing pH values, and the chemical shifts of the labeled carbon were recorded. For a single ionizing system where HA dissociates to H^+ and A^-, the observed ^{13}C chemical shift is given by eq 1

$$\delta = P_{HA}\delta_{HA} + P_{A-}\delta_{A-} \quad (1)$$

where δ_{HA} and δ_{A-} are the chemical shifts of species HA and A^-, respectively, while P_{HA} and P_{A-} are the populations of HA and A^- at a given pH, respectively. Equation 1 can be converted into eq 2, which expresses the relationship between the observed ^{13}C chemical shift and the acid dissociation constant of the hydrate.

$$\delta = \frac{\delta_{HA} + (\delta_{A^-}K_a)/[H^+]}{1 + K_a/[H^+]} \quad (2)$$

The pH dependence of the ^{13}C chemical shift for AcLF−^{13}CH(OH)$_2$ is given in Figure 5. The signal moves from 92.9 ppm at low pH to 97.4 ppm at high pH ($\Delta\delta$ = 4.5 ppm). A fit of the chemical shift data to eq 2 gives a pK_a value of 13.3, similar to that of 13.5 for acetaldehyde hydrate. This is about 4 log units higher than the corresponding value for the hydrate of AcLF-CF_3 (*25*). The difference is due to the inductive effect of the CF_3 group, which is strongly electron withdrawing.

A hemiacetal of AcLF-CHO, such as the Ser 195 adduct, will display a higher value of pK_a than the hydrate because of the statistical factor—either of two protons can dissociate from the hydrate but only one from a hemiactal—provided that the inductive effects at OR and OH groups are essentially the same. The statistical factor corresponds to 0.3 log unit,

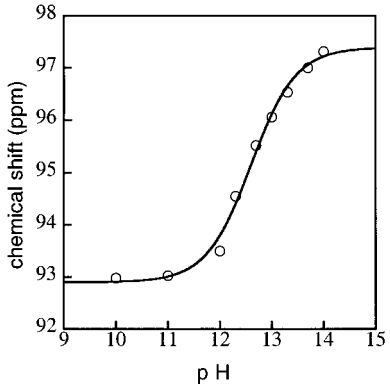

FIGURE 5: pH titration of hydrated AcLF-^{13}CH(OH)$_2$. The observed ^{13}C chemical shifts are plotted here as a function of pH to illustrate the change upon ionization of AcLF-^{13}CH(OH)$_2$ to AcLF-^{13}CH(OH)-O$^-$. The curve represents the fit of the points to eq 2, which yields a pK_a of 13.3 for the aldehyde hydrate.

so an ordinary hemiacetal of AcLF-CHO would display a pK_a of 13.6, assuming no difference in electronic effects between the hydrate and hemiacetal. In an effort to determine the pK_a of the methyl hemiacetal AcLF-CH(OH)OCH$_3$, ^{13}C NMR spectra of the aldehyde in methanol and water (80/20, v/v) were obtained. The chemical shift of the hemiacetal was found to be 99.92 ppm. However, the instability of the compound in extremely basic solutions prevented the determination of the high pK_a value. A further complication is that the pK_a of a hemiacetal in an 80/20 (v/v) methanol/water mixture is 0.6 unit higher than it would be in water, owing to the greater polarity of water than methanol (*25*). This effect would drive the pK_a in the methanol/water mixture to 14.2. The instability of AcLF-CHO in such basic solutions is likely to be related to enolization, peptide ionization, and solvolysis.

^{13}C NMR Signal for the Chymotrypsin−AcLF-CHO Adduct. The adduct of AcLF-^{13}CHO with chymotrypsin displays a signal at 102 ppm in neutral solutions. A study of the effect of pH on this signal showed very little change between pH 7.0 and 13.0. The signal drifted gradually from 102.0 ppm at pH 7 to 102.7 ppm at pH 13. The results could not be attributed to an ionization of the hemiacetal functional group. As discussed above, the value of pK_a for a hemiacetal of AcLF-CHO in water is expected to be ~13.6, so in these experiments we would not have detected the ionization unless the interaction of the hemiacetal hydroxyl group with the oxyanion binding site had stabilized the anionic form enough to decrease the pK_a to less than 13.

Ionic Structure of the Adduct of Chymotrypsin and AcLF-CHO. In the hemiketal complexes of chymotrypsin with AcLF-CF$_3$, His 57 is protonated at pHs as high as 12.0, and the proton bridging His 57 and Asp 102 displays a chemical shift of 18.9 ppm (*2*, *3*, *25*). In marked contrast, the downfield region of the ^{1}H NMR spectra of the chymotrypsin−AcLF-CHO adduct in neutral solutions show that His 57 is not ionized.

The neutrality of His 57 in the hemiacetal adduct raised the question of the protonation and charge state of the hemiacetal oxygen. If it is anionic, as in the hemiketal adducts of peptidyl trifluoromethyl ketones, the reaction should proceed with release of the proton from Ser 195. To determine whether a hydronium ion is released or taken up with complexation, the pHs of solutions of unbuffered

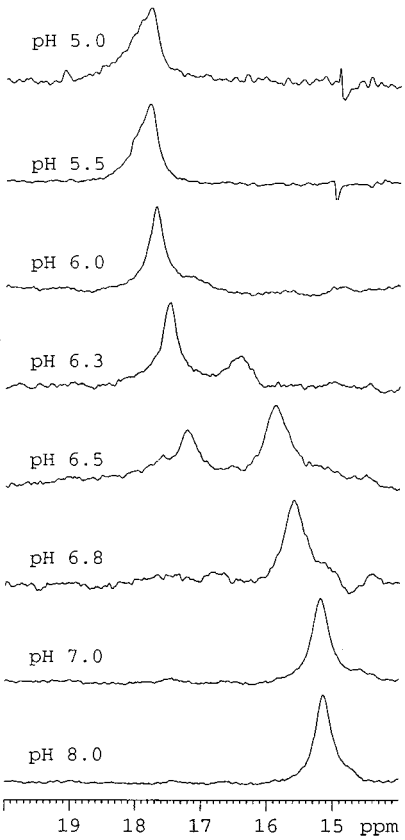

FIGURE 6: Effects of pH on the downfield ^{1}H NMR spectra of the chymotrypsin−AcLF-CHO complex.

chymotrypsin at 1 mM at four pHs between 3 and 8 were monitored with the stepwise addition of AcLF-CHO from 0.2 to 2.0 mM in 8−10 additions. In no case could any change in pH be detected upon addition of the inhibitor. The measured pHs were 3.29 ± 0.03, 4.74 ± 0.01, 7.17 ± 0.01, 7.27 ± 0.01, and 7.52 ± 0.01. If 1 equiv of acid had been released upon complexation, 1 mM hydronium ion would have been produced, and the measured pH would have decreased accordingly. In a control experiment, addition of 1 mM HCl to 1 mM chymotrypsin at pH 7.55 resulted in a pH of 7.16. The control proved that the release of 1 equiv of hydrogen ions upon complexation would have been detected. Therefore, the reaction of chymotrypsin with AcLF-CHO must be isoprotonic, as is its reaction with AcLF-CF$_3$ (*17*). The simplest disposition of the proton from Ser 195 in an isoprotonic mechanism would be as in eq 3, retention on the hemiacetal oxygen.

$$\text{AcLF-CHO} + \text{HO}-\text{Ser}^{195}\text{-Cht} \rightarrow \text{AcLF-C(OH)O}-\text{Ser}^{195}\text{-Cht} \quad (3)$$

Ionization of His 57 in the Chymotrypsin−AcLF-CHO Adduct. The downfield regions of the ^{1}H NMR spectra of the chymotrypsin−AcLF-CHO adduct at pHs ranging from 8.0 to 5.0 are shown in Figure 6. At pH >7.0, the downfield proton appears at 15.1 ppm, corresponding to unprotonated His 57. At pH <6.3, the downfield proton moves to 17.8 ppm, corresponding to protonated His 57. The titration is complex because of the appearance of intermediate downfield species at pH 6.3 and 6.5. A plot of the chemical shifts against pH, taking the intermediate species into account, is shown in Figure 7. The titration curve is steep and fits an

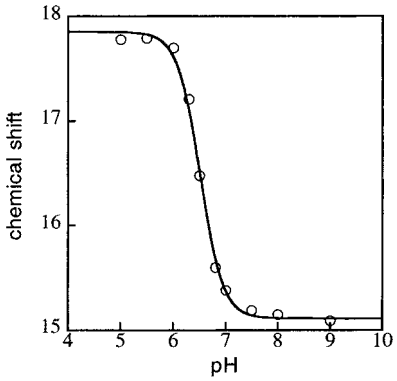

FIGURE 7: pH titration of His 57 in the hemiacetal complex of chymotrypsin with AcLF-CHO. Shown are the downfield proton chemical shifts in Figure 6 plotted against pH for the chymotrypsin−AcLF-CHO complex as a function of pH. At pH 6.3 and 6.5, the weighted averages of chemical shifts of the two peaks were used for the plot. The curve is calculated for a pK_a of 6.5 and an ionization requiring two protons, one for His 57 and one for an unidentified group that ionizes in concert with His 57. The ionic state of the other group affects the chemical shift of His 57. Similar ionization behavior is displayed by free chymotrypsin, but with a pK_a of 7.5 (*26*, *27*).

ionization equation corresponding to the cooperative dissociation of two protons. The fitted curve is for a pK_a value of 6.51. The ionization of His 57 in the chymotrypsin−AcLF-CHO complex is analogous to that of free chymotrypsin, which also displays intermediate species and a steep titration curve (*26*, *27*). The pK_a value for free chymotrypsin is 7.5.

DISCUSSION

Structures of Chymotrypsin−Inhibitor Complexes. The resolution of the structures of the hemiketal complexes of chymotrypsin with AcF-CF_3 is extended to 1.4 Å, and the close contacts between Nδ1 of His 57 and Oδ1 of Asp 102 are reconfirmed at the higher resolution. These close contacts are a necessary condition for LBHB formation, and these conditions are present in the structures. Spectroscopic and chemical evidence for the presence of LBHBs in these and other peptidyl trifluoromethyl ketone adducts of chymotrypsin has been presented (*1*−*4*, *28*). The evidence included downfield ^{1}H NMR signals at 18.6−18.9 ppm for the proton bridging His 57 and Asp 102, low deuterium fractionation factors of 0.3−0.4 ppm, high pK_a values of 10.6−12 for His 57, high activation energies (13−19 kcal mol^{-1}) for exchange of the downfield protons with water, and a deuterium isotope effect on the NMR chemical shift of the downfield signal.

The structure of the hemiacetal adduct of chymotrypsin with AcLF-CHO is similar to those of the trifluoromethyl ketone adducts with the exception of the placement of the hemiacetal oxygen. In the trifluoromethyl ketone adducts, the hemiketal oxygen is confined to the oxyanion binding site. However, AcLF-CHO forms two adducts with Ser 195, one with the *S*-configuration at the hemiacetal carbon and the oxygen in the oxyanion site and another with the *R*-configuration and the oxygen hydrogen bonded to Nϵ2 of His 57. The stereoisomerism raised the question of the electrostatic charge on the hemiacetal oxygen. Inasmuch as His 57 is unprotonated at pH >7, and the addition of AcLF-CHO to Ser 195 is isoprotonic, it appears that the hemiacetal is neutral as in eq 3. Neutrality of the hemiacetal accounts for partial occupancy of the oxyanion binding site.

Dual sites for the hemiacetal oxygen in other complexes of peptidyl aldehydes with serine proteases have been described but not explained (*9*−*11*). The other peptidyl hemiacetal adducts were probably also neutral and not attracted to the oxyanion site. The chemical basis for neutrality of the hemiacetal oxygen in the adduct of chymotrypsin with AcLF-CHO is its high basicity, as shown below. This is likely to be the case whenever an enzyme is inhibited by nucleophilic addition of an amino acid side chain to an aldehyde.

Ionic States of His 57 in Inhibitor−Carbonyl Complexes of Chymotrypsin. Chemical structures **1** and **2** represent the addition complexes of chymotrypsin with AcLF-CHO and AcLF-CF_3, respectively. In addition to the substitution of H in the hemiacetal for CF_3 in the hemiketal, they differ in the placement of the proton liberated from Ser 195. In the adduct with AcLF-CHO, the proton is bonded to the hemiacetal oxygen, and in that of AcLF-CF_3, it is bonded to His 57.

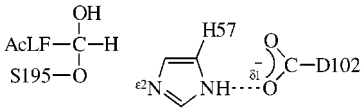

1

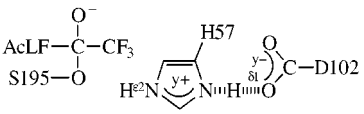

2

In the AcLF-CF_3 complex of chymotrypsin, His 57 is protonated at pH <12 (pK_a = 12) (*2*, *3*). Inasmuch as the pK_a of His 57 ranges from 10.6 to 12, depending on the structure of the peptidyl moiety, it is reasonable to expect His 57 to be as basic in structure **1** (from AcLF-CHO) as in **2** (from AcLF-CF_3). However, in structure **1** the hemiacetal oxyanion is even more basic (pK_a $\approx$ 13.6). Therefore, in the competition between His 57 and the hemiacetal for the proton released from Ser 195, the hemiacetal oxygen acquires the proton. Reaction of AcLF-CF_3 with chymotrypsin to form the hemiketal adduct with Ser 195 is also isoprotonic, and complex formation is also accompanied by competition for the proton from Ser 195. In that case, the pK_a of the methyl hemiketal of AcLF-CF_3 in aqueous solution is 9.1, and lower in the active site, while that of His 57 is 12 so that His 57 is protonated.

Weak Interactions at the Oxyanion Binding Site. The neutrality of the hemiacetal oxygens in adducts of peptidyl aldehydes with Ser 195 of serine proteases explains only the partial occupancy of the oxyanion binding site. However, this raises the question of why the oxyanion binding sites do not lower the pK_as of the adducts enough to allow them to be anionic. The oxyanion binding site is widely regarded as the principal stabilizing interaction of tetrahedral intermediates in catalysis. A strongly stabilizing oxyanion site should decrease the pK_a value of a hemiacetal to less than 12, the pK_a of His 57 in such complexes. This would correspond to only 2.5 kcal mol^{-1} in free energy at 25 °C. It would lead to structures analogous to that of a peptidyl trifluoromethyl ketone adduct, with the oxyanion of the adduct in its binding site and His 57 protonated. However,

Table 3: Ionization Energetics of Groups in Chymotrypsin and Peptide Tetrahedral Adducts

Species of Cht	Ionizing group	pK_a	$\lvert\Delta\Delta G^\circ\rvert$ (kcal mol^{-1})[a]
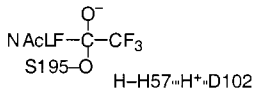	Hemiketal–OH	5[b]	6.3
	His 57-Nε2	12[c]	7.3
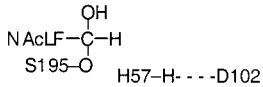	Hemiacetal–OH	>13[d]	- -
	His 57-Nε2	6.5[d]	0.4
S195–OH H57–H- - - -D102	His 57-Nε2	7.5[e]	0.98

[a] The absolute value of $\Delta\Delta G^\circ$ is calculated from the difference in the values of pK_a for the group in chymotrypsin and the same group in aqueous solution. [b] From ref *25*. [c] From refs *2* and *3*. [d] From this work. [e] From refs *26* and *27*.

no such stabilization is observed in the peptidyl aldehyde complexes of serine proteases.

In this context, it is worth noting that the apparent pK_a of the analogous hemiketal hydroxyl group in the complex of AcLF-CF_3 with chymotrypsin has been reported to be lower than 5, or 4.5 log units lower than the pK_a of the methyl hemiketal in aqueous solution (*25*). Much of this difference, 6.3 kcal mol^{-1} in free energy, has been attributed to oxyanion stabilization at its binding site. Why is there so little stabilization of the hemiacetal adducts? The structures are the same except for the weak binding to the oxyanion site. All things considered, the observations of protonated, neutral peptidyl hemiacetal adducts at the active sites of serine proteases re-open the question of the degree of oxyanion stabilization afforded by the oxyanion binding sites.

Mutational analysis of oxyanion stabilization in chymotrypsin is very difficult because the hydrogen bond donors are the main chain NH groups of Gly 193 and Ser 195, which cannot easily be altered. Efforts in this direction have been more successful in studies of subtilisin, in which the side chain of Asn 155 contributes one of the hydrogen bond donors in the oxyanion binding site. Decreases in kinetic reactivity of 80−300-fold have been reported when this residue was mutated to Gly, Ala, or Leu (*29*−*31*). These are modest but significant effects, corresponding to 2.5−3.3 kcal mol^{-1} in transition state destabilization. Because of auxiliary effects of the mutations, the kinetically evaluated effects on the transition states should be regarded as *maximum* estimates of the stabilization afforded by the side chain of Asn 155. A stabilizing effect of 2.5−3.0 kcal mol^{-1} in the hemiactetal adduct of chymotrypsin with AcLF-CHO should have been detected in the pH dependence of the ^{13}C NMR signal but was not.

An Empirical Rule for Ionizations at the Active Site. It is difficult to sort out the many microenvironmental effects on the ionization constants of individual functional groups at enzymatic active sites. The available data on chymotrypsin adducts with AcLF-CF_3 and AcLF-CHO are assembled in Table 3. In the AcLF-CF_3 adduct, both the hemiketal oxygen and Nϵ2 of His 57 display grossly perturbed pK_a values relative to the values of the same functional groups in solution. Elevation of the pK_a of His 57 and depression of that of the hemiketal can be understood on the basis that any change in the overall electrostatic charge in the site must surmount an energy barrier. In Table 3, this barrier is defined as the absolute difference in free energy of ionization in the active site relative to the equivalent ionization in aqueous solution, and it is expressed as $\lvert\Delta\Delta G^\circ\rvert$. The values of $\lvert\Delta\Delta G^\circ\rvert$ are in the range of 6−7 kcal mol^{-1}, both for the addition and for the loss of a proton from the site.[2]

The overall electrostatic charge in the AcLF-CHO complex is the same as in the AcLF-CF_3 complex, although both His 57 and the hemiacetal oxygen are not ionized at pH >7. The hemiacetal-OH group displays no tendency to ionize below pH 13, which is consistent with the barrier to altering the overall charge in the site. His 57, however, undergoes ionization with a pK_a of ∼6.5 to form a strong hydrogen bond with Asp 102. While this ionization changes the net charge in the active site, it does not encounter a high energy barrier. Similarly, His 57 in free chymotrypsin undergoes ionization with a pK_a value of 7.5 (*26*, *27*), also with a small value of $\lvert\Delta\Delta G^\circ\rvert$. Why do these ionizations not encounter large energy barriers? It may be that they would were it not for the stabilization afforded by the strong hydrogen bonds, possibly LBHBs, that accompany the protonation of His 57. In this model, stabilization by strong hydrogen bonding compensates for the barrier against altering the electrostatic charge in the active site. Ionizations that do not increase hydrogen bond strength must overcome the barrier to changing the net electrostatic environment.

The hydrogen bonds between His 57 and Asp 102 in the protonated forms of chymotrypsin and of its adduct with AcLF-CHO are characterized by downfield ^{1}H NMR signals at 17.7 ppm. These signals are significantly upfield from the corresponding signal at 18.9 ppm of the adduct formed

[2] Liang and Abeles offered a different rationale for the low value of pK_a in the ionization of the hemiketal hydroxyl group (*25*). They suggested that electrostatic stabilization by His 57 and hydrogen bonding in the oxyanion binding site might account for the acidity of this group. The present results do not support an important role for the oxyanion binding site. Moreover, in proposing electrostatic stabilization by His 57 at a range of 5.5 Å, Liang and Abeles did not consider the effect of the negative charge of Asp 102 on His 57 at a distance of only 2.6 Å.

between chymotrypsin and AcLF-CF_3 (*1*−*4*). Extensive evidence of LBHB formation between His 57 and Asp 102 in the latter case has been presented, including extreme deshielding of the bridging proton, as observed in NMR experiments (*1*−*3*), a very low deuterium fractionation factor (*4*), a very high activation enthalpy for exchange with medium protons (*4*), and a positive deuterium isotope effect on the chemical shift of the bridging proton (*28*). Analogous data on the proton bridging His 57 and Asp 102 in free chymotrypsinogen at low pH indicated strong hydrogen bonding as well (*32*), although perhaps not as strong as that in the AcLF-CF_3 adduct. Analogous data are not available for the protonated adduct of AcLF-CHO with chymotrypsin; however, the similarity of the downfield proton with that in protonated chymotrypsinogen suggests that it may also be strongly hydrogen bonded.

The foregoing hypothesis for the impact of an LBHB upon protonation of His 57 revises an earlier theory that the binding of a peptidyl group leads, through a small conformational change, to compression between Nδ1 of His 57 and Oδ1 of Asp 102 (*2*, *3*). In the new hypothesis, the compression already exists in the structure of chymotrypsin and is not brought about by peptide binding or LBHB formation upon protonation of His 57. The compression facilitates LBHB formation and enhances the basicity of His 57 in processes that do not lead to net changes in the overall electrostatics of the active site. These processes include the addition of Ser 195 to a peptide carbonyl group in the transition state and the analogous addition to transition state analogues such as peptidyl trifluoromethyl ketones.

The foregoing hypothesis for the effects of the LBHB in the active site of chymotrypsin can in principle be tested experimentally. If it is correct, disruption of the LBHB by a means that does not alter the overall electrostatic charge in the site should have predictable effects on the ionizing properties of His 57. Consider, for example, the replacement of Asp 102 with a residue that is isoelectrostatic and nearly isosteric with aspartate but cannot form an LBHB with His 57 owing to mismatched proton affinities. Then the protonation of His 57 in free chymotrypsin might not be accompanied by LBHB formation, and His 57 might display a lower pK_a value. This change might also alter the charge distribution in the adduct of AcLF-CF_3 with chymotrypsin. Future studies should be designed to test these ideas critically.

SUPPORTING INFORMATION AVAILABLE

Electronic structure of bis(iminobenzosemiquinonato)metal (Cu, NI, or Pd) complexes. This material is available free of charge via the Internet at http://pubs.acs.org.

REFERENCES

1. Frey, P. A., Whitt, S. A., and Tobin, J. B. (1994) *Science 264*, 1927−1930.
2. Cassidy, C. S., Lin, J., and Frey, P. A. (1997) *Biochemistry 36*, 4576−4584.
3. Lin, J., Cassidy, C. S., and Frey, P. A. (1998) *Biochemistry 37*, 11940−11948.
4. Lin, J., Westler, W. M., Cleland, W. W., Markley, J. L., and Frey, P. A. (1998) *Proc. Natl. Acad. Sci. U.S.A. 95*, 14664−14668.
5. Hibbert, F., and Emsley, J. (1990) *Adv. Phys. Org. Chem. 26*, 255−379.
6. Jeffrey, G. A. (1997) *An Introduction to Hydrogen Bonding*, Oxford University Press, New York.
7. Hammond, G. S. (1955) *J. Am. Chem. Soc. 77*, 334.
8. Brady, K., Wei, A., Ringe, D., and Abeles, R. H. (1990) *Biochemistry 29*, 7600−7607.
9. Delbaere, L. T. J., and Brayer, G. D. (1985) *J. Mol. Biol. 183*, 89−103.
10. James, M. N. G., Sielecki, A. R., Brayer, G. D., and Delbaere, L. T. J. (1980) *J. Mol. Biol. 144*, 43−88.
11. Kurinov, I. V., and Harrison, R. W. (1996) *Protein Sci. 5*, 752−758.
12. Stoddard, B. L., Bruhnke, J., Porter, N., Ringe, D., and Petsko, G. A. (1990) *Biochemistry 29*, 4871−4879.
13. Kabsch, W. (1988) *J. Appl. Crystallogr. 21*, 71.
14. Cohen, G. H., Silverton, W., and Davies, D. R. (1981) *J. Mol. Biol. 148*, 449.
15. Tronrud, D. E., Ten Eyck, L. F., and Mathews, B. W. (1987) *Acta Crystallogr. A43*, 489−501.
16. Brunger, A. T., Kuriyan, J., and Karplus, M. (1987) *Science 235*, 458−460.
17. Imperiali, B., and Abeles, R. H. (1986) *Biochemistry 25*, 3760−3767.
18. Higuchi, N., Saitoh, M., Niwata, S., Kiso, Y., and Hayashi, Y. (1995) U.S. Patent 5,395,824.
19. Hore, P. J. (1983) *J. Magn. Reson. 55*, 283−300.
20. Luzatti, P. V. (1952) *Acta Crystallogr. 5*, 802−810.
21. Breaux, E. J., and Bender, M. L. (1975) *FEBS Lett. 56*, 81−84.
22. Chen, R., Gorenstein, D. G., Kennedy, W. P., Lowe, G., Nurse, D., and Schultz, R. M. (1979) *Biochemistry 18*, 921−926.
23. Thompson, R. C. (1973) *Biochemistry 12*, 47−51.
24. Brady, K., and Abeles, R. H. (1990) *Biochemistry 29*, 7608−7617.
25. Liang, T.-C., and Abeles, R. H. (1987) *Biochemistry 26*, 7603−7608.
26. Robillard, G., and Shulman, R. G. (1974) *J. Mol. Biol. 76*, 541−558.
27. Zhong, S., Haghjoo, K., Kettner, C., and Jordan, F. (1995) *J. Am. Chem. Soc. 117*, 7048−7055.
28. Cassidy, C. S., Lin, J., and Frey, P. A. (2000) *Biochem. Biophys. Res. Commun. 273*, 789−792.
29. Bryan, P., Pantoliano, M. W., Quill, S. F., Hsiao, H. Y., and Poulos, T. (1986) *Proc. Natl. Acad. Sci. U.S.A. 83*, 3743−3745.
30. Whiting, A. K., and Peticolas, W. L. (1994) *Biochemistry 33*, 552−561.
31. O'Connell, T. P., Day, R. M., Torchilin, E. V., Bachovchin, W. W., and Malthouse, J. G. (1997) *Biochem. J. 326*, 861−866.
32. Markley, J. L., and Westler, W. M. (1996) *Biochemistry 35*, 11092−11097.

BI002535A